Ultrastructural analysis of sequential Cyprinid herpesvirus 3 morphogenesis *in vitro*

Sean J. Monaghan*[a], Sven M. Bergmann[b], Kim D. Thompson[c], Linton Brown[a], Tharangani Herath[d], Jorge del-Pozo[e], Alexandra Adams[a]

[a] Institute of Aquaculture, School of Natural Sciences, University of Stirling, Stirling, FK9 4LA, UK s.j.monaghan@stir.ac.uk; lintonbrown@hotmail.com; alexandra.adams@stir.ac.uk

[b] Friedrich-Loeffler- Institut, Südufer 10, 17493 Greifswald, Insel-Riems, GERMANY Sven.Bergmann@fli.bund.de

[c] Moredun Research Institute, Pentlands Science Park, Bush Loan, Midlothian, UK, EH26 0PZ Kim.Thompson@moredun.ac.uk

[d] Department of Animal Production, Welfare and Veterinary Sciences, Harper Adams University, Newport, Shropshire, UK, TF10 8NB therath@harper-adams.ac.uk

[e]The Royal (Dick) School of Veterinary Studies, University of Edinburgh, Easter Bush Campus, Midlothian, EH25 9RG Jorge.Del.Pozo@ed.ac.uk

* Corresponding author

Abstract

Cyprinid herpesvirus 3 (CyHV-3) is an alloherpesvirus, and the aetiological agent of koi herpesvirus disease. Although the complex morphogenic stages of the replication cycle of CyHV-3 were shown to resemble that of other members of the *Herpesvirales*, detailed analysis of the sequence and timing of these events was not definitively determined. This study describes these features through a time course using cyprinid cell cultures (KF-1 and CCB) infected with CyHV-3 (KHV isolate, H361) and analysed by transmission electron microscopy. Rapid viral entry was noted, with high levels of intracellular virus within 1-4 hours post-infection (hpi). Intra-nuclear capsid assembly, paracrystalline array formation and primary envelopment of capsids occurred within 4 hpi. Between 1-3 days post infection (dpi), intra-cytoplasmic secondary envelopment occurred, as well as budding of infectious virions at the plasma membrane. At 5-7 dpi, the cytoplasm contained cytopathic vacuoles, enveloped virions within vesicles, and abundant non-enveloped capsids; also there was frequent nuclear deformation. Several morphological features are suggestive of inefficient viral assembly, with production of non-infectious particles, particularly in KF-1 cells. The timing of this alloherpesvirus morphogenesis is similar to other members of the *Herpesvirales* but there may be possible implications of using different cell lines for CyHV-3 propagation.

Keywords: Cyprinid herpesvirus 3, CyHV-3, Koi herpesvirus (KHV), sequential morphogenesis, transmission electron microscopy (TEM)

Introduction

Cyprinid herpesvirus 3 (CyHV-3) is the official taxonomical classification of koi herpesvirus (KHV) (Waltzek *et al*. 2005), the highly virulent and economically important aetiological agent of koi herpesvirus disease (KHVD) (Hedrick *et al*. 2000; 2005). The virus has had a devastating impact on to the global koi and carp (*Cyprinus carpio* Linnaeus, 1758) aquaculture industries since outbreaks were first reported in Israel and the U.S. in 1998 (Hedrick *et al*. 2000; Perelberg *et al*. 2003). CyHV-3 is a member of the recently formed family *Alloherpesviridae* (Waltzek *et al*. 2005) in the order *Herpesvirales* (Davison *et al*. 2009). This classification has been based on the close phylogenetic relationship of the virus with CyHV-1 (Aoki *et al*. 2007; Waltzek *et al*. 2009), the causative agent of carp pox (Sano *et al*. 1991; 1992; Päak *et al*. 2011), CyHV-2; goldfish haematopoietic necrosis virus (GHNV) of goldfish (*Carassius auratus* Linnaeus, 1758) (Goodwin *et al*. 2006; 2009; Lovy & Friend 2014) and AngHV-1, causing herpesvirus disease in European eels (*Anguilla anguilla* Linnaeus, 1758) (Van Beurden *et al*. 2011; Armitage *et al*. 2014). Morphogenic stages of CyHV-3 have been shown to resemble those of other herpesviruses, both *in vitro* (Miwa *et al*. 2007) during cytopathic effects of CyHV-3 inoculated cells and *in vivo* (Miyazaki *et al*. 2008) during clinically diseased, experimentally challenged fish, expressing KHVD, supporting the designation of the virus as a herpesvirus (Hedrick *et al*. 2000). However, little is known with regards to the timing of the various stages of *Alloherpesviridae* virion maturation. As with other herpesviruses, CyHV-3 displays differential infection phases, including fatal lytic infection and potential latent infection (Gilad *et al*. 2003; 2004; St-Hilaire *et al*. 2005; Eide *et al*. 2011; Reed *et al*. 2014; Sunarto *et al*. 2014), which can be influenced by temperature (Ronen *et al*. 2003; St-Hilaire *et al*. 2005; Sunarto *et al*. 2014). These different infection states can impact serological and molecular detection sensitivities,

as limited antibodies or viral DNA copy numbers are produced during acute and latent infections, respectively (Bergmann *et al*. 2010; Matras *et al*. 2012; Monaghan *et al*. 2015). Despite the development of tools for CyHV-3 detection and progress made in understanding viral replication and stages of infection, most studies related to this virus have been based on molecular and antibody-based methodologies (Gilad *et al*. 2004; Pikarsky *et al*. 2004; Ilouze *et al*. 2012a; b; Monaghan *et al*. 2016). A potential pitfall of these approaches is that viral DNA concentrations and expressed antigen may not directly correlate with the number of infectious CyHV-3 particles, as virion particle formation may be incomplete. An example of this is the prototype of herpesviral replication, herpes simplex virus type 1 (HSV-1), where only around 25% of viral DNA and protein is considered to be assembled into virions (Ginsberg 1988). The kinetics of actual virion morphogenesis during replication is currently unknown for CyHV-3, and information relating to this cannot be obtained by using the techniques mentioned above.

Morphogenic stages of herpesviruses are complex, occurring partly in the nucleus (i.e. capsid assembly, packaging of replicated genome, primary envelopment and nuclear egress/de-envelopment) and in the cytoplasm (i.e. tegumentation, secondary envelopment and budding of infectious virions at the plasma membrane) (reviewed in Mettenleiter, 2002; Mettenleiter *et al*., 2009). Although the morphology of CyHV-3 has previously been shown to resemble that of other members of the *Herpesvirales*, detailed analysis of the sequence and timing of the events involved in virion production have not been fully determined for the *Alloherpesviridae*. The stages of CyHV-3 morphogenesis have been described in detail by Miwa *et al*. (2007) after 7 dpi including the formation of three capsid types during assembly in the nucleus and maturation and egress from the nucleus through two distinct envelopment events.

In the current study the stages of CyHV-3 morphogenesis were investigated from 1 hpi to 7 days post inoculation in two of the most commonly used cyprinid cell lines for CyHV-3 virus propagation, common carp brain (CCB) and koi fin (KF-1). The goal of the study was to evaluate inconsistencies that may occur between the cell lines with respect to virus maturation and cell pathology, as these can have potential implications for successful propagation of infectious CyHV-3 virus particles.

Materials and Methods

Cell culture

The KF-1 cells used in the study were developed from epidermal tissue of koi (Hedrick *et al*. 2000), and were kindly provided by Dr. Keith Way (Centre for Environment, Fisheries and Aquaculture Science (CEFAS), Weymouth, UK). The CCB cells were kindly provided by Dr. Matthias Lenk (Friedrich Loeffler Institut (FLI), Greifswald, Germany), and were developed from brain tissue of common carp (Neukirch *et al*. 1999). Both cell lines were cultured in Eagle's Minimum Essential Medium (EMEM) containing Eagles's salts (Invitrogen), 10 % foetal bovine serum (FBS), 1 % Non-Essential amino acids (NEAA, Invitrogen) and 2 mM L-glutamine at 22-25°C with 4 % CO_2. During all stages of the study, including optimisation of the KHV infection and harvest protocol for TEM analysis, the KF-1 cells were maintained between a subculture passage of 108–144 and CCB cells between passage 69-84.

Virus culture

The isolate of CyHV-3 (genotype U, KHV, H361) used in this study originated from an adult koi with clinical KHVD in Eastern USA in 1998 (Hedrick *et al*. 2000). Cell lines were sub-cultured and maintained at 22°C for a period of 24-36 h, until a monolayer of 50% or 70-80% confluence was obtained for KF-1 and CCB cells, respectively. At this point, the culture medium was removed and the monolayers were carefully washed with Dulbecco's phosphate

buffered saline (DPBS) prior to inoculating the cells with the virus. The KF-1 cells were inoculated with CyHV-3 at a multiplicity of infection (MOI) of 0.01 and CCB cells with an MOI of 0.02 from a virus stock of KHV $10^{4.4}$ tissue culture infectious dose (virus infection of 50 % inoculated cells ($TCID_{50}$)) mL^{-1}. An adsorption period of 1-2 h at 20°C was performed before re-supplementing the cultures with fresh EMEM (+2 % FBS). After a cytopathic effect (CPE) of 90–100 % was obtained, the virus was harvested by exposing the monolayer to two cycles of freeze-thawing at -70°C, and then centrifuging the lysed cell suspension at 3,800 x *g* (Eppendorf 5804 R). The clarified supernatant was collected and stored as aliquots at -70°C until used.

Virus quantitation

KF-1 and CCB cells were cultured overnight at 22°C in 24 or 96 well tissue culture plates (Nunc, Denmark) to form a monolayer. After the monolayers were 50-60 % confluent, the culture medium was removed and the cells were inoculated with 100 µL of a 5-fold serial dilution of the virus, diluted in Hank's buffered salt solution (HBSS), 2 % FBS. Mock infected cells were also included, which received only culture medium without virus. Virus was absorbed onto the cells for 1-2 h at 20°C, before re-supplementing the cells with fresh EMEM medium containing 2 % FBS. Cells were checked for the development of a CPE after 7 and 14 dpi. For calculating the initial virus inoculation dose the $TCID_{50}$ was determined according to the Spearman-Kärber method (Kärber 1931). Multiplicity of infection (MOI) was determined as described by Voronin *et al*. (2009).

Time course infection of cell lines

Nine tissue culture flasks ($75cm^2$) per cell line were used for time course analysis of CyHV-3 morphogenesis. KF-1 cultures were seeded at 5 x 10^6 cells $flask^{-1}$ and CCB cultures were seeded at 2 x 10^6 cells $flask^{-1}$. Cells were cultured for 24 h at 22°C prior to initiating the trial.

Two non-infected flasks per cell line were used as negative controls, which were sampled at 1 dpi and 7 dpi. For the seven test flasks, monolayers were inoculated with 3 mL KHV as described above, and sampled at 1, 4 and 8 hpi, and 1, 3, 5, and 7 dpi. Samples were taken by washing the monolayers twice with 10 mL DPBS, and then fixing the cells *in-situ* with 6 mL 2.5% glutaraldehyde (Sigma-Aldrich, UK) in 0.1M sodium cacodylate buffer, pH 7.3. Cells where then scraped into suspension using a rubber policeman and 6 mL (3 mL x 2) of the suspension were centrifuged at 2000 x *g* for 10 min at 4°C to form a pellet (slow speed centrifugation was used to avoid cell rupture). Pellets were post fixed with fresh 2.5% glutaraldehyde for 2-4 h or overnight at 4°C. The fixative was removed and 2 mL 0.1M sodium cacodylate buffer was added to the pellets, which were detached from the tube wall with a wooden applicator and stored at 4°C until processed.

Transmission Electron Microscope (TEM) processing and visualisation

Glutaraldehyde fixed cell pellets were post-fixed in 1 % osmium in 0.1M sodium cacodylate buffer in closed vials for 1 h at 22°C. The pellets were then washed for 3 x 10 min in distilled H_2O to remove the cacodylate buffer. This enabled 'En-bloc' staining of pellets with 2 % uranyl acetate in 30 % acetone in the dark for 1 h. This was followed by dehydration: 60 % acetone for 30 min, 90 % for 30 min, 100 % for 30 min then incubation in fresh 100 % acetone for 1 h. Pellets were then infiltrated with agar low viscosity resin (ALVR) on a rotator (Taab, UK). The pellets were first incubated with ALVR diluted 1:1 in acetone for 45 min followed by 100% ALVR for 1 h and then into fresh ALVR for another 1 h. The pellets were finally embedded in block moulds and polymerised in an oven at 60°C overnight. One hundred micron ultra-thin sections were prepared from the resin blocks using a microtome (Reichert Ultracut E, Leica, UK) with a diamond knife (Diatome, US) and placed on 200 µm mesh Formvar-coated copper grids. These were first stained with 4 % uranyl acetate in 50 % ethanol for 4 min, followed by Reynold's lead citrate for 7 min. The sections were examined

under an FEI Tecnai Spirit G2 Bio Twin Transmission Electron Microscope. Measurements of virions were made using FEI Tecnai software.

Results

TEM analysis of CyHV-3 morphogenesis in infected cells

Virus particle sizes differed depending on the stage of morphogenesis, the measured immature capsids (*n*=48) = 97.56 nm (SD± 8.78), nucleocapsids (*n*=16) = 114.12 nm (SD± 12.13), primary enveloped virions (*n*=5) = 138.32 nm (SD ±18.43) and secondary enveloped mature virions (*n*=18) = 167.97 nm (SD ±31.38), were all within the size range of CyHV-3 particles reported in the literature (Hedrick *et al*. 2005; Miwa *et al*. 2007; Miyazai *et al*. 2008). No discernible difference was noted in the sizes of virions obtained from the CCB cells or the KF-1 cells.

KHV in infected cells during the first 24 hpi

Many cells were devoid of virions and their ultrastructure was normal and similar to the control cells at this stage (Fig. 1 A). A small number of both CCB and KF-1 cells contained intranuclear paracrystalline capsid arrays at 4 hpi. This was associated with reduction of heterochromatin/euchromatin ratio and chromatin margination (Fig. 1 B and C). The capsids observed were predominantly devoid of electron dense cores, and were occassionally toroid (Fig. 1 B-D). The capsids observed within the paracrystalline arrays were predominantly toroid in appearance (Fig. 1 C). Lamellar bodies, reminiscent of lipofuscin, were occasionally observed regardless of the infection status (Fig. 1 B).

Between 4 hpi – 1 dpi, virus capsids were observed throughout the nucleus at various stages of maturation in a large number of the infected cells. Capsids were often located below the

inner nuclear envelope, occasionally featuring an envelope – primary envelopment (Fig. 1 E). Capsids with electron dense cores were more frequent at this stage.

By 1 dpi, naked nucleocapsids (without a secondary envelope) had assembled in the cytoplasm of infected cells, some contained an electron dense core, while others were empty (Fig. 1 F). A this stage, intracytoplasmic secondary enveloped particles within vesicles were already present, with nuclei harbouring large numbers of capsids as described above (Fig 1 F). There were no discernable differences in virion formation or cell pathology between KF-1 or CCB cells at this stage.

Figure 1 positioned here

CyHV-3 virus in infected cells at 3 dpi

At 3 dpi, although the frequency of infected cells had increased, the cells contained relatively few virus particles and many of the cells remained uninfected (Fig. 2 A). Mature virions could be observed in intracytoplasmic vesicles of CCB cells however, which also featured large, clear intracytoplasmic cytopathic vacuoles (Fig. 2 B-C). Extracellular virions were observed at this stage in KF-1, but not in CCB cells (Fig. 2 D). Rare abnormalities were apparent within the nucleus, with intra-nuclear vesicles in CCB cells suggestive of primary envelopment of empty capsids (Fig. 2 E). Capsids at various stages of maturation, including intranuclear paracrystalline arrays were common observations in both CCB and KF-1 cells at this time (Fig. 2 F).

Figure 2 positioned here

CyHV-3 virus in infected cells at 5 and 7 dpi

At 5 dpi there was a greater abundance of virus particles in both cell lines, at various stages of morphogenesis. Primary envelopment was clearly seen where sometimes ≥ three

nucleocapsids were contained within the perinuclear cisterna at one time (Fig. 3 A-B). At 5 dpi the occurrence of cytopathic vacuoles increased with some containing internalised mature enveloped virus particles, while other virions had budded into cytoplasmic vesicles, especially in CCB cells (Fig. 3 C). Mature virions were often observed associated with, and budding within, vesicles from the Golgi apparatus (Fig. 3 D) or from the cell membrane, which were sometimes in clumped, membrane bound extracellular aggregates (Fig. 3 E-F). While the majority of intracellular enveloped virus particles were observed in CCB cells, there were greater numbers of extracellular mature virions observed in TEM micrographs of infected KF-1 cells.

Figure 3 positioned here

Clusters of naked nucleocapsids were often found in close proximity to cytopathic vacuoles (Fig. 4 A), sometimes with protruding cores (Fig. 4B) and secondary enveloped mature virions within intracytoplasmic vesicles (Fig. 4 C). By this stage the compartments of the mature herpesvirus virion were clearly defined, including the projections of the glycoprotein envelope, amorphous tegument layer, capsid and electron-dense core (Fig. 4 D).

Figure 4 positioned here

Virion morphogenesis and egress at membranous compartments throughout the course of infection

As the infection of cells was not synchronised, it is not possible to determine the precise timing of various morphogenesis events at the cellular level. However, by 3 dpi all stages of morphogenesis had been observed, including docking of nucleocapsids at the nuclear pore (Fig. 5 A), primary envelopment resulting in both viable virions with electron dense cores (Fig. 5 B) and likely abberant capsidless intracisternal L-particles (Fig. 5 C). Budding of

tegumented capsids within Golgi-derived vesicles could be observed within the cytosol - secondary envelopment, often associated with deformation and fragmentation of these organelles (Fig. 5 D). Increased numbers of mature infectious virions were observed budding-off from the cell membrane from 3 dpi onwards, resulting in numerous extracellular mature virions (Fig. 5 E–F). No extracellular virions were observed during the first day of infection, suggesting that extracellular virions noted later were the result of viral replication in both CCB and KF-1 cells and not from inoculated virus.

Figure 5 positioned here

Cytopathologies / abnormalities in cells at late stages of CyHV-3 infection

The nuclei were often deformed at late infection stages with intra-nuclear vesicles and cytoplasmic invaginations (Fig. 6 A–B). Proliferating intra-nuclear membranes exhibiting thickening and folds were also noted in some cells, extending inwards from the inner nuclear leaflet (Fig. 6 C-D). Occasionally, these nuclear envelope changes were associated with extreme levels of immature capsid primary envelopment (Fig. 6 D). The nuclear membrane in these cells exhibited re-duplication as well as thickening of the inner leaflet (Fig. 6 A & D). On rare occasions apparently disrupted nuclear membranes were observed resulting in loose folds surrounded by putative nucleocapsids or capsid-like structures at various stages of maturation (Fig. 6 E–F). Both CCB and KF-1 cells exhibited nuclear deformations, but greater numbers of capsids were observed in the affected CCB cells.

Figure 6 positioned here

Discussion

The morphogenesis of CyHV-3 has been described in some detail in cultured cyprinid cells NGF-2 (epithelial-like cells from the fins of coloured carp) (Miwa *et al*. 2007), and in

255 infected carp (Miyazaki *et al*. 2008), however, analysis was only undertaken after 7 dpi. In
256 the current study the sequence of morphological development of the CyHV-3 virion from 1
257 hour through to 7 days post inoculation was examined, together with the cell changes
258 associated with CyHV-3 infection in CCB and KF-1 cells.

259 One of the most notable findings of the investigation, not previously reported, was the
260 presence of capsids within the cell nucleus at various stages of maturation within the first 4
261 hpi. DNA replication of other herpesviruses, as measured using molecular methods, is
262 initiated as early as 3 hpi (Ben-Porat & Veach 1980), and Dishon *et al*. (2007) and Ilouze *et*
263 *al*. (2012b) demonstrated that CyHV-3 DNA synthesis occurs between 4-8 hpi in CyHV-3-
264 infected CCB cells. Capsid assembly does not occur until late mRNAs have been translated
265 and the structural proteins incorporated into the nucleus. Pseudorabies virus (PrV) and
266 channel catfish virus (CCV) capsids, for example, were not detected in the nucleus of
267 infected cells until 4 hpi (Wolf & Darlington 1971; Granzow *et al*. 1997). Transcripts of
268 genes coding proteins involved in CyHV-3 maturation and assembly were not observed by
269 Ilouze *et al*. (2012a) until 4-8 hpi. It has also been shown that there is no expression of
270 structural proteins encoded by ORF149 or 84 (an envelope glycoprotein and capsid-
271 associated protein, respectively) at this stage of the infection (Monaghan *et al*. 2016).
272 Monoclonal antibodies and polyclonal anti-sera to specific CyHV-3 antigens have now been
273 produced (Rosenkranz *et al*. 2008; Aoki *et al*. 2011; Dong *et al*. 2011; Fuchs *et al*. 2014),
274 which may facilitate further studies on CyHV-3 virion replication and maturation in cultured
275 cells. For example it would be possible to confirm the timing of production of capsids using
276 immunofluorescence or immuno-gold TEM by detecting capsid-associated proteins, e.g. with
277 antibodies recognising antigens expressed by ORF84 or ORF92 (Dong *et al*. 2011;
278 Monaghan *et al*. 2016).

279 The characteristics of CyHV-3 capsid assembly have been previously described by Miwa *et*
280 *al*. (2007), including the most abundant type of virion consisting of two concentric circles
281 (the inner containing heterogenous material, thought to be capsomers and scaffolding protein
282 in PrV (Granzow *et al*. 1997)), a second type with an electron dense core and a third type that
283 is empty. By harvesting infected cell cultures during the first day of inoculation it was
284 possible to determine the earlier capsid formation type in our study which was similar to that
285 described for the third type described by Miwa *et al*. (2007). These were similar to those
286 previously described for avian and mammalian herpesviruses by Nii (1991) being mostly
287 empty with no electron dense core or toroid in appearance, and thus were likely to lack DNA
288 at this stage. This is supported by the absence of more mature virions in the cells at this early
289 stage of infection.

290 Due to the low MOI used in the study, i.e. 0.01–0.02, many cells were uninfected at this early
291 stage ($\leq$ 4 hpi). However, where cells were infected, virus particles were predominantly
292 observed within the nucleus. Due to the short window for virus replication post-inoculation in
293 cells harvested at 4 hpi, this study confirms that these phases of virion formation, also
294 reported by Miwa *et al*. (2007), occurred within those 4 hours of infection. Therefore, like
295 other herpesviruses, absorption of infectious virus particles to the cell, translocation of
296 capsids to the nucleus and subsequent initiation of capsid assembly of CyHV-3 appears to be
297 rapid. In mammalian herpesvirus infection experiments, shifting of PrV infected cells from
298 non-permissive to permissive temperatures resulted in virion attachment to the cell membrane
299 within 1 min and intracellular importation of virions after only 5 min (Granzow *et al*. 1997).
300 Imported PrV nucleocapsids are found in close proximity to microtubules, and had
301 sometimes already docked at the nuclear pore within 30 min (Granzow *et al*. 1997; Kaelin *et*
302 *al*. 2000). This was not observed in the current study thus may have been missed as cells

were only harvested from 1 hpi or could possibly be due to the low MOI, which limited the infection to a relatively small proportion of cells, although electron dense capsids were found at the nuclear pore of some cells later in the experiment. Although viropexis via coated pits has been observed in the cell membrane in early infection stages of PrV (Granzow *et al*. 1997), Brogden *et al*. (2015) recently provided evidence to suggest that CyHV-3 infection of CCB cells is facilitated via lipid rafts. To determine this at the ultrastructural level, temperature manipulation of CyHV-3 inoculated cells would have to be performed using a higher MOI, similar to the studies carried out for PrV and HSV-1 (Granzow *et al*. 1997; Klupp *et al*. 2000; Nicola *et al*. 2003; Abaitua *et al*. 2012). Nonetheless, coated pits were observed in infected cells in the current study in close proximity to possible naked nucleocapsids (not shown). These may have been migrating towards the nuclear pores, although no microtubules were observed near these. Interestingly, electron dense and electron lucent virus-like particles were observed in linear arrays, some in close proximity to the nuclear envelope within the first 4 hpi. These resembled capsids and were observed at later stages of infection in cells with disrupted nuclei (7 dpi), but the lack of electron density of some of these structures suggests that no DNA was present to be released at the nuclear pore, or perhaps had already been released.

As mentioned above, the capsids observed within the nucleus during the first day of infection exhibited all 3 stages of maturation, similar to findings for other herpesviruses (Nii *et al*. 1968; Wolf & Darlington 1971; Nii 1991; Granzow *et al*. 1997). In addition to this, primary envelopment of nucleocapsids was also observed during the first day of infection, with no envelopment observed within the cytoplasm. Despite using a non-synchronised infection model in the current study, all infected cells analysed during the first day after inoculation were infected for < 1 dpi, suggesting that an eclipse stage of the infection was still ensuing, as

mature extracellular infectious enveloped virions were absent until > 1 dpi (i.e. there was no production of infectious particles evident (Flint *et al*. 2009)). However, secondary envelopment was reported from 12-14 hpi with mammalian herpesviruses PrV and HSV-1 (Mettenleiter, 2004), and nucleocapsids could be seen budding within intracytoplasmic vesicles by 1 dpi with CyHV-3 in the current study.

Within the first day of infection cytopathic changes were observed including nuclear hypertrophy and margination of chromatin. This is similar, although not as rapid as the chromatin margination and initiation of syncytia reported after only 2 hpi in cells infected with another member of the *Alloherpesviridae*, CCV (Wolf & Darlington 1971). This is not surprising as infectious progeny virus can be isolated from CCV infected catfish after only 1 dpi (Kancharla & Hanson 1996) compared to the lag time of CyHV-3 infected carp (i.e. > 3dpi from blood leukocytes, Matras *et al*., 2012). This may correspond to differences in viral replication kinetics between different alloherpesviruses, which unlike members of the *Herpesviridae*, express different optimal temperature ranges between fish species (Hansen *et al*. 2011).

The formation of paracrystalline-like arrays of intra-nuclear capsids had previously been reported within the nucleus of infected carp gill epithelial cells (Hedrick *et al*. 2000), and in the cytoplasm of a more recently developed koi caudal fin cell line (KCF-1) (Dong *et al*. 2011), and this study revealed that this occurs within just 4 hpi in both CCB and KF-1 cells.. These arrays are typical of herpesvirus infected cells (Nii *et al*. 1968; Granzow *et al*. 1997). These have been described as pseudocrystals in PrV infected cells, which are hypothesised to dissolve during replication and release individual capsids as they are not found in necrotic cells following replication (Granzow *et al*. 1997). The current study supports this as these

capsid formations were no longer observed after 3 dpi, despite being found in a relatively large number of cells prior to this.

In contrast to the rapid production of progeny virus of the alloherpesvirus, CCV within 10-12 hpi (Wolf & Darlington 1971), release of extracellular infectious virions appears much slower for CyHV-3 and other herpesviruses (i.e. 3-5 dpi) as shown from their growth curves (Ahlqvist *et al*. 2005; Dishon *et al*. 2007; Costes *et al*. 2008; 2009; Dong *et al*. 2011). Although infectious titre ($TCID_{50}$) was not measured at each time point in the current study, an increase in production of infectious secondary enveloped virions was observed after 3 dpi by ultrastructural analysis. Dishon *et al*. (2007) also reported that 3-7 days are required for progeny virus to be released from CyHV-3 infected CCB cells at the permissive temperature as measured by qPCR. Later in the infection all stages of virus morphogenesis could be observed and the size of capsids, nucleocapsids, primary enveloped and secondary enveloped virions were in agreement with other TEM studies on CyHV-3 and other allopherpesviruses (Wolf & Darlington 1971; Hedrick *et al*. 2000; 2005; Miwa *et al*. 2007; Miyazaki *et al*. 2008). In a recent study, there was elevated expression and abundance of capsid-associated protein after 1 dpi compared to envelope glycoprotein (Monaghan *et al*. 2016). This corresponds with fewer secondary enveloped (mature) virions, i.e. containing envelope glycoproteins, during early infection stages, compared to abundant non-enveloped capsids and nucleocapsids observed throughout the infection. With other herpesviruses, aberrant particles are able to leave the cell through exocytosis (Granzow *et al*. 1997), thus they may increase the production of non-infectious particles. Production of infectious CyHV-3 particles in cell culture may be similar to other herpesviruses for which only ~100 virus particles may be infectious out of a total of ~10^4-10^5 particles (Ginsberg 1988). More extracellular virions appeared to be present in the KF-1 cells compared to the CCB cells, however, the presence of

enveloped virions within intracytoplasmic vesicles or budding off from the trans-golgi network (TGN) appeared more prominent in CCB cells. These differences may have implications with regards to the production of high titre virus stocks, as KF-1 cells appeared more prone to lysis (Pers obs.) and thus reduced their potential for producing mature virus particles. For example, after 5-7 dpi, aggregates of extracellular mature enveloped virus particles were apparent in the KF-1 cells, which were likely defective. Further studies using immuno-labelling methods for tegument proteins such as ORF62 (Aoki *et al*. 2011) or membrane proteins ORF81 and ORF149 (Rosenkranz *et al*. 2008; Fuchs *et al*. 2014) could elucidate more definitively the tegumentation and envelopment / de-envelopment processes of CyHV-3 morphogenesis.

Lamellar bodies were observed in the cytoplasm of both infected and control cells, reminiscent of lipofuscin, a change associated with cell aging. These aging cells are likely to have been passaged on to the subcultured monolayers inoculated in the trial, and the lamlellar bodies should therefore not be considered as a pathology related with herpesvirus infection. However, a number of nuclear deformations were observed after 5–7 dpi, that were not observed in non-infected control cells, thus were likely to be associated with elevated virus production and infection and not the senescence of old cells.

Miwa *et al*. (2007) also commented on the finding of compartment-like structures in CyHV-3 infected NGF-2 cell nuclei after 7 dpi, but without specific details. A high competition between nucleocapsids for budding, via the perinuclear envelope and intracytoplasmic vesicles of the TGN observed in the current study, may have contributed not only to these irregular formations found within the nuclear envelope, but also other deformed organelles and the formation of syncytia. Miyazaki *et al*. (2008) reported on the degeneration of organelles during later stages of CyHV-3 infection in carp cells. The re-duplication of the

nuclear envelope, intra-nuclear folds and incorporated vesicles may occur in herpesvirus infected cells through the accumulation of virus-derived antigens within the cisternae, partly due to virions acquiring the inner nuclear envelope during primary envelopment (Miyazaki *et al*. 2008). Similar formations are found in alphaherpesviruses, where primary enveloped virions accumulate in the perinuclear region in the absence of proteins that are required for successful egress and further maturation (Granzow *et al*. 2004). This can result in thickening (Ghadially 1997) leading to nuclear envelope proliferations, fusions and subsequent abnormal concentric lamellar structures (Nii *et al*. 1968). These are characteristic cytopathologies observed in CyHV-3 and other herpesviruses (Nii *et al*. 1968; Wolf & Darlington 1971; Nii 1991; Ghadially 1997; Miwa *et al*. 2007). Disrupted nuclei in the current study contained not only nuclear envelope proliferations in both cell lines, but also occasionally CCB cells contained intra-nuclear vesicles, which were more pronounced at later stages of infection and sometimes resembled those reported in CyHV-3 infected carp cells by Miyazaki *et al*. (2008). In contrast to the results reported by Miwa *et al*. (2007), primary envelopment within the nuclear envelope was observed more often at the later stages of infection. Furthermore, the production of capsidless particles in the perinuclear envelope, possibly intracisternal L-particles, as previously reported for alphaherpesviruses by Granzow *et al*. (2001), may lead to inefficient viral assembly, and also contribute to the production of non-infectious particles following increased viral infection pressure. Formation of syncytia on the other hand, is thought to result from mutations in glycoprotein genes (Pereira 1994), with an extensive production of intracellular mature and immature virus particles, which with CyHV-3 occurred more often in CCB cells than KF-1 cells, probably due to the latter being more prone to lysis. Syncytial formation has previously been described in CyHV-3 infected CCB cells (Adamek *et al*. 2012), which also occurred in the current study with viral particles possibly released gradually through budding instead of cell lysis. As a result of cell lysis there may have been a

greater loss of virus from KF-1 cells as non-infectious particles, although budding events at the cell plasma membrane of KF-1 cells was observed. The greater loss of virus particles from KF-1 cells by 7 dpi may also explain why only few particles were observed in the KF-1 cell line in the study by Miwa *et al*. (2007).

Cytopathic vacuoles have been noted in KHV infected cells after 7 dpi (Miwa et al., 2007), however, by analysing infected cells at different times post-inoculation an increased abundance of these vacuoles was observed between 5–7 dpi compared with earlier time points. These cytopathic vacuoles contained infectious virus particles in CCB cells to a greater extent than KF-1 cells. These may be associated with vacuolation (i.e. CPE) at this later stage of the infection, as reported in other studies (Dishon *et al*. 2007), which is possibly as a result of competitive budding processes occurring with increased infectious virus progeny. This can be explained by either fusion of a large number of secretory vesicles, or many virions budding through limited golgi-derived vesicles (Granzow *et al*. 1997), which increases over the course of infection in the presence of greater numbers of mature infectious virions, later resulting in fragmentation and damage in the cytoplasm. However, synchronised infection experiments using higher MOI would be required to determine the actual time at which these formations occur and whether they're due to competitive budding.

In conclusion, sequential ultrastructural analysis of CyHV-3 morphogenesis within the first day post-inoculation revealed rapid formation of capsids, including paracrystalline array formation, within the first 4 hpi. Assessment of morphogenic stages from 1 – 7 dpi indicated that by 1 dpi CyHV-3 virions undergo primary and secondary envelopment and virion maturation is complete, but it is not until 3-5 dpi that abundant mature infectious virions are produced. These mature infectious particles bud off via the cell plasma membrane, sometimes in defective aggregates, but often resulting in accumulated infection levels in adjacent cells.

Such high infection levels may result in deformations in the cell, such as nuclear envelope reduplication and vast vacuolation and subsequent production of non-infectious, as well as infectious virus particles. In the current study this was evident at the ultrastructural level as abundant non-enveloped nucleocapsids and capsids compared to enveloped particles. KF-1 cells appear more prone to lysis, possibly releasing immature particles and non-infectious particles, whereas more virus particles are retained in CCB cells for complete maturation and budding at the cell plasma membrane. This should be taken into account when propagating CyHV-3 in CCB and KF-1 cells for the production of infectious virus.

Acknowledgements

This study was funded by MSD Animal Health and University of Stirling as part of SJ Monaghan's Ph.D Programme. The authors would like to thank Ms. Katherine Fiona Muir at the Virology unit of the Institute of Aquaculture, University of Stirling, UK for her invaluable technical support.

References

Abaitua F., Hollinshead M., Bolstad M., Crump C.M. & O'Hare P. (2012) A nuclear localization signal in the herpesvirus protein VP1-2 is essential for infection via capsid routing to the nuclear pore. *Journal of Virology* **86**(17), 8998-9014.

Adamek M., Rakus K.Ł., Chyb J., Brogden G., Huebner A., Irnazarow I. & Steinhagen D. (2012) Interferon type I responses to virus infections in carp cells: *In vitro* studies on *Cyprinid herpesvirus 3* and *Rhabdovirus carpio* infections. *Fish and Shellfish Immunology* **33**, 482-493.

Ahlqvist J., Fotheringham J., Akhyani N., Yao K., Fogdell-Hahn A. & Jacobson S. (2005) Differential tropism of human herpesvirus 6 (HHV-6) variants and induction of latency by HHV-6A in oligodendrocytes. *Journal of Neurovirology* **11**, 384-394.

Aoki T., Hirono I., Kurokawa K., Fukuda H., Nahary R., Eldar A., Davison A.J., Waltzek T.B., Bercovier H. & Hedrick R.P. (2007) Genome sequences of three koi herpesvirus isolates representing the expanding distribution of an emerging disease threatening koi and common carp worldwide. *Journal of Virology* **81**, 5058-5065.

Aoki T., Takano T., Unajak S., Takagi M., Kim Y.R., Park S.B., Kondo H., Hirono I., Saito-Taki T., Hikima J.-I. & Jung T.S. (2011) Generation of monoclonal antibodies specific for ORF68 of koi herpesvirus. *Comparative Immunology, Microbiology and Infectious Diseases* **34**, 209-216.

Armitage J., Hewlett N.R., Twigg M., Lewin N.C., Reading A.G., Williams C.F., Aprahamian M., Way K., Feist W. & Peeler E.J. (2014) Detection of *herpesvirus anguillae* during two mortality investigations of wild European eel in England: implications for fishery management. *Fisheries Management and Ecology* **21**(1), 1-12.

Ben-Porat T. & Veach R.A. (1980) Origin of replication of the DNA of a herpesvirus (pseudorabies). *Proceedings of the National Academy of Sciences* **77**, 172-175.

Bergmann S.M., Riechardt M., Fichtner D., Lee P. & Kempter J. (2010) Investigation on the diagnostic sensitivity of molecular tools used for detection of Koi herpesvirus. *Journal of Virological Methods* **163**(2), 229-233.

Brogden G., Adamek M., Proepsting M.J., Ulrich R., Naim H.Y. & Steinhagen D. (2015) Cholesterol-rich lipid rafts play an important role in the Cyprinid herpesvirus 3 replication cycle. *Veterinary Microbiology* **179**, 204-212.

Costes B., Fournier G., Michel B., Delforge C., Raj V.S., Dewals B., Gillet L., Drion P., Body A., Schynts F., Lieffrig F. & Vanderplasschen A. (2008) Cloning of the Koi herpesvirus genome as an infectious bacterial artificial chromosome demonstrates that disruption of the thymidine kinase locus induces partial attenuation in *Cyprinus carpio koi*. *Journal of Virology* **82**(10), 4955-4964.

Costes B., Raj V.S., Michel B., Fournier G., Thirion M., Gillet L., Mast J., Lieffrig F., Bremont M. & Vanderplasschen A. (2009). The major portal of entry of koi herpesvirus in *Cyprinus carpio* is the skin. *Journal of Virology* **83**(7), 2819-30.

Davison A.J., Eberle R., Ehlers B., Hayward G.S., McGeoch D.J., Minson A.C., Pellet P.E., Roizman B., Studdert M.J. & Thiry E. (2009) The order Herpesvirales. *Archives of Virology* **154**, 171-177.

Dishon A., Davidovich M., Ilouze M. & Kotler M. (2007) Persistence of *Cyprinid herpesvirus 3* in infected cultured carp cells. *Journal of Virology* **81**(9), 4828-4836.

Dong C., Weng S., Li W., Li X., Yi Y., Liang Q. & He J. (2011) Characterisation of a new cell line from caudal fin of koi, *Cyprinus carpio koi*, and first isolation of cyprinid herpesvirus 3 in China. *Virus Research* **161**, 140-149.

Eide K.E., Miller-Morgan T., Heidel J.R., Kent M.L., Bildfell R.J., LaPatra S., Watson G. & Jin L. (2011) Investigation of koi herpesvirus latency in koi. *Journal of Virology* **85**(10), 4954-4962.

Flint S.J., Enquist L.W., Racaniello V.R. & Skalka A.M. (2009). Principles of Virology, Volume II: Pathogenesis and Control, Chapter 4: Immune Defenses, 3rd Edition, ASM Press, pp. 87-132.

Fuchs W., Granzow H., Dauber M., Fichtner D. & Mettenleiter T.C. (2014). Identification of structural proteins of koi herpesvirus. *Archives of Virology* **159**(12), 3257-3268.

Fuchs W., Veits J., Helferich D., Granzow H., Teifke J.P. & Mettenleiter T.C. (2007) Molecular biology of avian infectious laryngotracheitis virus. *Veterinary Research* **38**, 261-279.

Ghadially F. (1997). Mitochondria. *In* Ultrastructural pathology of the cell and matrix, Fourth Edition, (Ghadially F. Ed.) Butterworth-Heinemann **1**: 195-328.

Gilad O., Yun S., Adkison M.A., Way K., Willits N.H., Bercovier H. & Hedrick R.P. (2003) Molecular comparison of isolates of an emerging fish pathogen, koi herpesvirus, and the effect of water temperature on mortality of experimentally infected koi. *Journal of General Virology* **84**, 2661-2668.

Gilad O., Yun S., Zagmutt-Vergara F.J., Leutenegger C.M., Bercovier H. & Hedrick R.P. (2004) Concentrations of a Koi herpesvirus (KHV) in tissues of experimentally infected *Cyprinus carpio* koi as assessed by real-time TaqMan PCR. *Diseases of Aquatic Organisms* **60**, 179-187.

Ginsberg H.S. (1988) Herpesviruses. *In* Virology, (Dulbecco R. and Ginsberg H.S. Eds.), Second Edition, J. B. Lippincott Co. Chapter 53, pp. 161-177.

Goodwin A.E., Merry G.E. & Sadler J. (2006) Detection of the herpesviral hematopoietic necrosis disease agent (Cyprinid herpesvirus 2) in moribund and healthy goldfish: validation of a quantitative PCR diagnostic method. *Diseases of Aquatic Organisms* **69**(2-3), 137-143.

Goodwin A.E., Sadler J., Merry G.E. & Marecaux E.N. (2009) Herpesviral heamatopoietic necrosis virus (CyHV-2) infection: case studies from commercial goldfish farms. *Journal of Fish Diseases* **32**(3), 271-278.

Granzow H., Klupp B.G., Fuchs W., Veits J., Osterrieder N. & Mettenleiter T.C. (2001) Egress of alphaherpesviruses: Comparative ultrastructural study. *Journal of Virology* **75**(8), 3675-3684.

Granzow H., Klupp B.G. & Mettenleiter T.C. (2004) The pseudorabies virus US3 protein is a component of primary and of mature virions. *Journal of Virology* **78**, 1314-1323.

Granzow H., Weiland F., Jöns A., Klupp B.G., Karger A. & Mettenleiter T.C. (1997) Ultrastructural analysis of the replication cycle of Pseudorabies virus in cell culture: A reassessment. *Journal of Virology* **71**(3), 2072-2082.

Hansen L., Dishon A. & Kotler M. (2011) Herpesviruses that infected fish. *Viruses* **3**, 2160-2191.

Hedrick R.P., Gilad O., Yun S.C., McDowell T.S., Waltzek T.B., Kelley G.O. & Adkison M.A. (2005) Initial isolation and characterization of a herpes-like virus (KHV) from koi and common carp. *Bulletin of the Fisheries Research Agency* **2**, 1–7.

Hedrick R.P., Gilad O., Yun S., Spangenberg J.V., Marty G.D., Nordhausen R.W., Kebus M.J., Bercovier H. & Eldar A. (2000) A herpesvirus associated with mass mortality of juvenile and adult koi, a strain of common carp. *Journal of Aquatic Animal Health* **12**, 44-57.

Ilouze M., Dishon A. & Kotler M. (2012a) Coordinated and sequential transcription of the cyprinid herpesvirus-3 annotated genes. *Virus Research* **169**, 98-106.

Ilouze M., Dishon A. & Kotler M. (2012b) Down-regulation of the cyprinid herpesvirus-3 annotated genes in cultured cells maintained at restrictive high temperature. *Virus Research* **169**, 289-295.

Kaelin K., Dezélée S., Masse M.J., Bras F. & Flamand A. (2000) The UL25 protein of Pseudorabies virus associates with capsids and localises to the nucleus and to microtubules. *Journal of Virology* **74**(1), 474-482.

Kancharla S.R. & Hanson L. (1996) Production and shedding of channel catfish virus (CCV) and thymidine kinase negative CCV in immersion exposed channel catfish fingerlings. *Diseases of Aquatic Organisms* **27**, 25-34.

Kärber G. (1931) Beitrag zur kollectiven Behandlung pharmakologischer Reihenversuche. Naunyn-Schmiedeberg's *Archives of Pharmacology* **162**(4), 480-483.

Klupp B.G., Granzow H. & Mettenleiter T.C. (2000) Primary envelopment of pseudorabies virus at the nuclear membrane requires the UL34 gene product. *Journal of Virology* **74**, 10063-10073.

Klupp B.G., Granzow H., Mundt E. & Mettenleiter T.C. (2001) Pseudorabies virus UL37 gene product is involved in secondary envelopment. *Journal of Virology* **75**(19), 8927-8936.

Lovy J. & Friend S.E. (2014) Cyprinid herpesvirus-2 causing mass mortality in goldfish: applying electron microscopy to histological samples for diagnostic virology. *Diseases of Aquatic Organisms* **108**(1), 1-9.

Matras M., Antychowicz J., Castric J. & Bergmann S.M. (2012) CyHV-3 infection dynamics in common carp (*Cyprinus carpio*) – evaluation of diagnostic methods. *Bulletin of the Veterinary Institute in Pulawy* **56**, 127-132.

Mettenleiter T.C. (2002) Herpesvirus assembly and egress. *Journal of Virology* **76**(4), 1537-1547.

Mettenleiter T.C. (2004) Budding events in herpesvirus morphogenesis. *Virus Research* **106**(2), 167-180.

Mettenleiter T.C., Klupp B.G. & Granzow H. (2009) Herpesvirus assembly: An update. *Virus Research* **143**(2), 222-234.

Miwa S., Ito T. & Sano M. (2007) Morphogenesis of koi herpesvirus observed by electron microscopy. *Journal of Fish Diseases* **30**, 715-722.

Miyazaki T., Kuzuya Y., Yasumoto S., Yasuda M. & Kobayashi T. (2008) Histopathological and ultrastructural features of koi herpesvirus (KHV)-infected carp *Cyprinus carpio*, and the morphology and morphogenesis of KHV. *Diseases of Aquatic Organisms* **80**(1), 1-11.

Monaghan S.J., Thompson K.D., Adams A. & Bergmann S.M. (2015) Sensitivity of seven PCRs for early detection of koi herpesvirus in experimentally infected carp (*Cyprinus carpio* L.) by lethal and non-lethal sampling methods. *Journal of Fish Diseases* **38**(3), 303-319.

Monaghan S.J., Thompson K.D., Bron J.E., Bergmann S.M., Jung T.S., Aoki T., Muir K.F., Dauber M., Reiche S., Chee D., Chong S.M., Chen J. & Adams A. (2016) Expression of immunogenic structural proteins of Cyprinid herpesvirus 3 *in vitro* assessed using immunofluorescence. *Veterinary Research* **47**(1), 8.

Neukirch M., Böttcher K. & Bunnajirakul S. (1999) Isolation of a virus from koi with altered gills. *Bulletin of the European Association of Fish Pathologists* **19**(5), 221-224.

Nicola A.V., McEvoy A.M. & Straus S.E. (2003) Roles for endocytosis and low pH in herpes simplex virus entry into HeLa and Chinese hamster ovary cells. *Journal of Virology* **77**, 5324-5332.

Nii S. (1991) Electron microscopic study on the development of herpesviruses. *Journal of Electron Microscopy* **41**, 414-423.

Nii S., Morgan C. & Rose H.M. (1968) Electron microscopy of herpes simplex virus: II. Sequence of development. *Journal of Virology* **2**, 517-536.

Päak P., Hussar P., Järveots T. & Paaver T. (2011) Club cells active role in epidermal regeneration after skin hyperplasia of koi carp *Cyprinus carpio*. *AACL Bioflux* **4**(4), 455-462.

Pereira L. (1994) Function of glycoprotein B homologues of the family Herpesviridae. *Infectious Agents and Disease* **3**, 9-28.

Perelberg A., Smirnov M., Hutoran M., Diamant A., Bejerano Y. & Kotler M. (2003) Epidemiological description of a new viral disease afflicting cultured Cyprinus carpio in Israel. *The Israeli Journal of Aquaculture – Bamidgeh* **55**(1), 5-12.

Reed A.N., Izume S., Dolan B.P., LaPatra S., Kent M., Dong J. & Jin L. (2014) Identification of B cells as a major site for Cyprinid herpesvirus 3 latency. *Journal of Virology* **88**(16), 9297-9309.

Ronen A., Perelberg A., Abramowitz J., Hutoran M., Tinman S., Bejerano I., Steinitz M. & Kotler M. (2003) Efficient vaccine against the virus causing a lethal disease in cultured *Cyprinus carpio*. *Vaccine* **21**, 4677-4684.

Rosenkranz D., Klupp B.G., Teifke J.P., Granzow H., Fichtner D., Mettenleiter T.C. & Fuchs W. (2008). Identification of envelope protein ORF81 of koi herpesvirus. *Journal of General Virology* **89**, 896-900.

Sano N., Sano M., Sano T. & Hondo R. (1992). *Herpesvirus cyprini*: detection of the viral genome by in situ hybridisation. *Journal of Fish Diseases* **15**, 153-162.

Sano T., Morita N., Shima N. & Akimoto M. (1991) *Herpesvirus cyprini*: lethality and oncogenicity. *Journal of Fish Diseases* **14**, 533-543.

St-Hilaire S., Beevers N., Way K., Le Deuff R.M., Martin P. & Joiner C. (2005) Reactivation of koi herpesvirus infections in common carp *Cyprinus carpio*. *Diseases of Aquatic Organisms* **67**, 15-23.

687 Sunarto A., McColl K.A., Crane M.S.J., Schat K.A., Slobedman B., Barnes A.C. & Walker
688 P.J. (2014) Characteristics of Cyprinid herpesvirus 3 in different phases of infection:
689 Implications for disease transmission and control. *Virus Research* **188**, 45-53.
690
691 Tu C., Lu Y.P., Hsieh C.Y., Huang S.M., Chang S.K. & Chen M.M. (2014) Production of
692 monoclonal antibody against ORF72 of koi herpesvirus isolated in Taiwan. *Folia*
693 *Microbiology (Praha)* **59**(2), 159-165.
694
695 Van Beurden S.J., Leroy B., Wattiez R., Haenen O.L.M., Boeren S., Vervoort J.M., Peeters
696 B.P.H., Rottier P.J.M., Engelsma M.Y. & Vanderplasshen A.F. (2011). Identification and
697 localization of the structural proteins of anguillid herpesvirus 1. *Veterinary Research* **42**, 105-
698 120.
699
700 Voronin Y., Holte S., Overbaugh J. & Emerman M. (2009) Genetic drift of HIV populations
701 in culture. *PloS Genetics* **5**(3), e1000431.
702
703 Vrancken R., Boutier M., Ronsmans M., Reschner A., Leclipteux T., Lieffrig F., Collard A.,
704 Mélard C., Wera S., Neyts J., Goris N. & Vanderplasschen A. (2013) Laboratory validation
705 of a lateral flow device for the detection of CyHV-3 antigens in gill swabs. *Journal of*
706 *Virological Methods* **193**, 679-682.
707
708 Waltzek T.B., Kelley G.O., Alfaro M.E., Kurobe T., Davison A.J. & Hedrick R.P. (2009)
709 Phylogenetic relationships in the family Alloherpesviridae. *Diseases of Aquatic Organisms*
710 **84**, 179-194.
711
712 Waltzek T.B., Kelley G.O., Stone D.M., Way K., Hanson L., Fukuda H., Hirono I., Aoki T.,
713 Davison A.J. & Hedrick R.P. (2005) Koi herpesvirus represents a third cyprinid herpesvirus
714 (CyHV-3) in the family Herpesviridae**.** *Journal of General Virology* **86**, 1659-1667.
715
716 Wolf K. & Darlington R.W. (1971) Channel catfish virus: a new herpesvirus of ictalurid fish.
717 *Journal of Virology* **8**, 525-533.
718

Figures

Figure 1. TEM micrographs of CCB and KF-1 cells infected with Koi herpesvirus 1–24 hpi. (A) Uninfected CCB cell; (B) Infected KF-1 cells 4 hpi with paracrystalline formation of capsids in the nucleus; (C) High mag. of capsids shown in square of B; (D) Nucleus of infected CCB cells; (E) 2 infected CCB cells in close proximity 4 hpi. Note the accumulation of capsids towards the periphery of the diffuse cell nucleus with varying degree of maturation. Primary enveloped virions can also be observed; (F) Infected CCB cells after 1 dpi showing the formation of capsids within the nucleus and cytoplasm and mature virions that have a acquired a secondary envelope in the cytoplasm (Magnified in box). *N* = Nucleus; *C* = Cytoplasm; pca = Paracrystalline array; lbd = lamellar bodies; Arrow = capsids; Arrow heads = Enveloped virions; pev = Primary enveloped virions; sev = Secondary enveloped virions.

Figure 2. TEM micrographs of CCB and KF-1 cells infected with Koi herpesvirus 1–3 dpi. (A) CCB cells inoculated with KHV but uninfected; (B) Infected CCB cells with mature secondary enveloped virions; (C) High magnification of mature secondary enveloped virion (shown in square of B) within a vesicle in the cytoplasm; (D) Severely damaged KF-1 cells with budding infectious enveloped mature virion on cell membrane; (E) CCB cells with KHV showing intranuclear vesicles; (F) Infected KF-1 cell with paracrystalline array of capsids formed within the nucleus. *N* = Nucleus; *C* = Cytoplasm; pca = Paracrystalline array; Arrow = capsids; Arrow heads = Enveloped virions; cv = Cytopathic vacuole; inv = Intranuclear vesicle; ecv = Extracellular virion.

Figure 3. TEM micrographs of CCB and KF-1 cells infected with Koi herpesvirus 5–7 dpi. (A) Infected CCB cells containing capsids at various maturational stages in the nucleus and nucleocapsids budding through the nuclear envelope and acquiring a primary envelope. (B) High magnification of square in D showing 3 primary enveloped virions within the nuclear envelope while smaller immature and mature capsids remain in the nucleus. (C) Low magnification of infected CCB cells, 5 dpi, with a number of cytopathic vacuoles and secondary enveloped mature virions budding from various membranous organelles. (D) Mature secondary enveloped virion within the cell cytoplasm, budding from golgi apparatus derived vesicle in CCB cells, 7 dpi. (E) Infected KF-1 cells, 5 dpi with many mature secondary enveloped virions budding through the cell membrane. (F) High mag. of square in C showing aggregates of extracellular, mature, infectious secondary enveloped virions. *N* = Nucleus; *C* = Cytoplasm; Arrow = capsids; Arrow heads = Enveloped virions; pev = Primary enveloped virion; cv = Cytopathic vacuole; g = Golgi body; ecv = Extracellular virion.

Figure 4. TEM micrographs of CCB and KF-1 cells infected with Koi herpesvirus 5–7 dpi. (A) CCB cells with KHV – Many cytoplasmic nucleocapsids in close vicinity to vacuoles; (B) Clusters of naked/unenveloped capsids in the cytoplasm of infected CCB cells after 7 dpi. Note the protruding core into the cytoplasm; (C) Infected KF-1 cells, 7 dpi, containing secondary enveloped mature virions within cytoplasmic vesicles. Large cytopathic vacuoles are also evident containing cell debris; (D) High magnification of mature secondary enveloped virion in infected CCB cells, 5 dpi – note the defined layers: glycoprotein envelope with surface projections, tegument layer, capsid and electron dense core. *N* = Nucleus; *C* = Cytoplasm; Arrow = capsids; Arrow heads = Enveloped virions; cv = Cytopathic vacuole; icv = Intracytoplasmic vesicle; g = Golgi body; ecv = Extracellular virion.

Figure 5. TEM micrographs of CyHV-3 virion morphogenesis and egress at membranous compartments. (A) Infected CCB cells showing a nucleocapsid at a nuclear pore; (B) Infected CCB cells with KHV with electron dense nucleocapsid within the nuclear envelope; (C) Infected CCB cell with electron-lucent nucleocapsid (intracisternal L-particles) within the nuclear envelope; (D) Infected CCB cell containing a tegumented nucleocapsid budding in an inctracytoplasmic vesicle; (E) Infected CCB cell showing enveloped virion in the process of budding-off from the cell membrane; (F) Infected CCB cells with many secondary enveloped mature infectious virions in the extracellular space at later stages of infection. *N* = Nucleus; *C* = Cytoplasm; Arrow = capsids; Arrow heads = Enveloped virions; np = nuclear pore; pev = primary enveloped virion; clp = capsidless intracisternal L-particle; icv = intracytoplasmic vesicle; ecv = Extracellular virion.

Figure 6. TEM micrographs of CCB and KF-1 cells infected with Koi herpesvirus 5–7 dpi showing various cytopathologies.

(A) Infected KF-1 cells containing large vacuoles and large vesicle within the nuclear membrane; (B) CCB cells exhibiting a large intranuclear vesicle protruding inwards from the nuclear membrane containing putative disrupted virus particles after 7 dpi; (C) Infected KF-1 cells containing intranuclear folds; (D) Infected CCB cell after 7 dpi exhibiting proliferation of the inner membrane of the nuclear envelope surrounded by immature virus particles at various stages of maturation; (E) Disrupted nucleus of infected CCB cell exhibiting loose disrupted nuclear membrane with electron dense and electron luscent capsid-like structures present; (F) Higher mag. of E showing naked electron dense and empty capsid-like structures released from the disrupted nucleus. *N* = Nucleus; *C* = Cytoplasm; Arrow = capsids; inv = Intranuclear vesicle; inf = Intranuclear folds; dnm = Disrupted nuclear membrane.

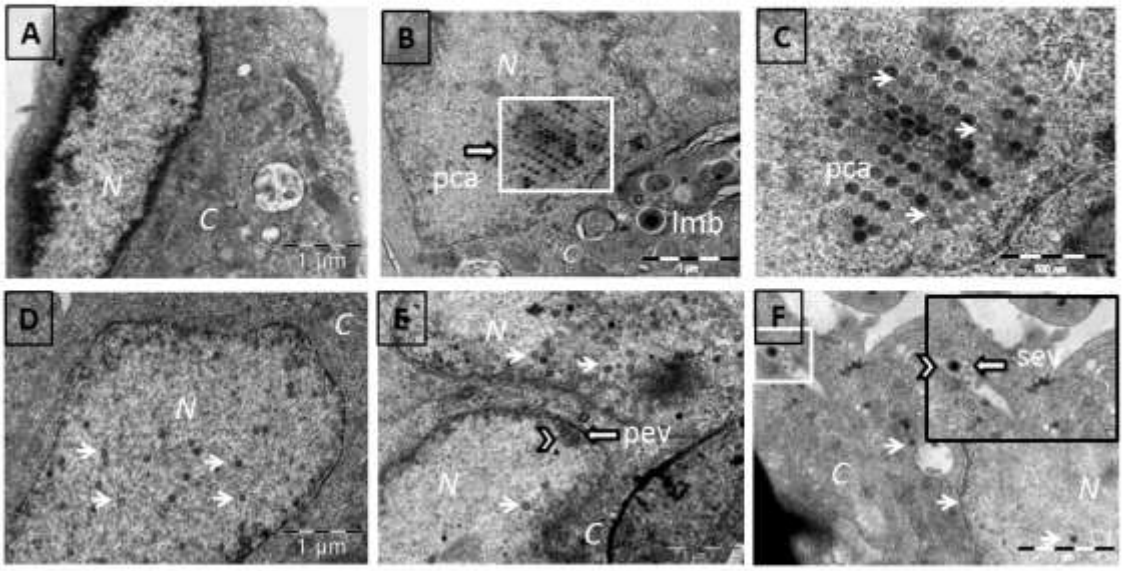

791

792 **Figure 1. TEM micrographs of CCB and KF-1 cells infected with Koi herpesvirus 1–24 hpi.**

793

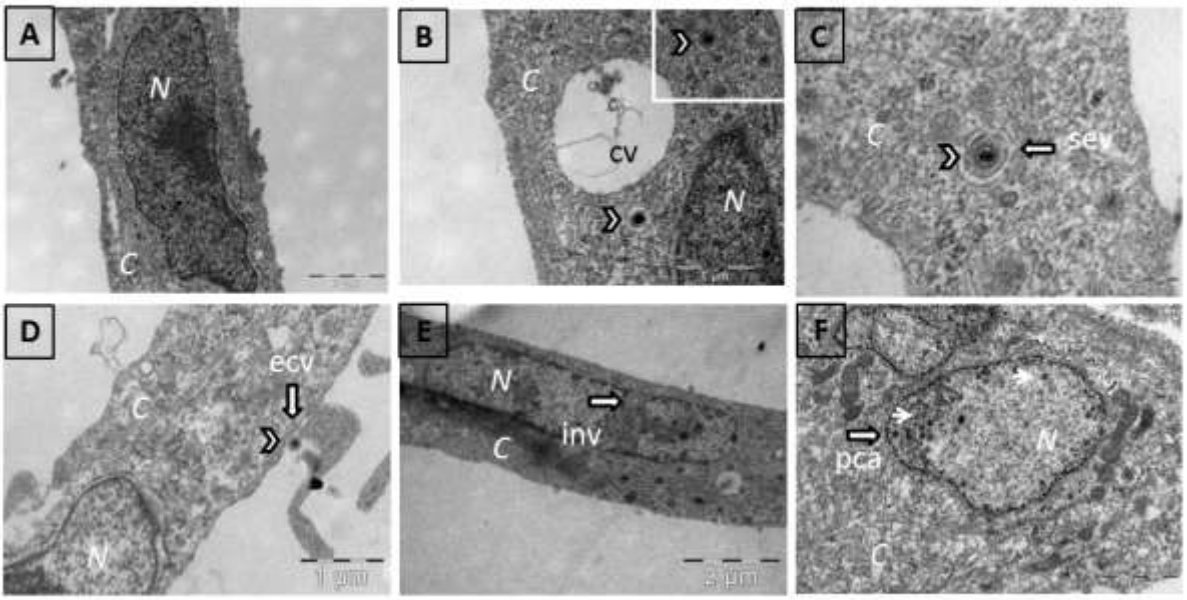

794

795 **Figure 2. TEM micrographs of CCB and KF-1 cells infected with Koi herpesvirus 1–3 dpi.**

796

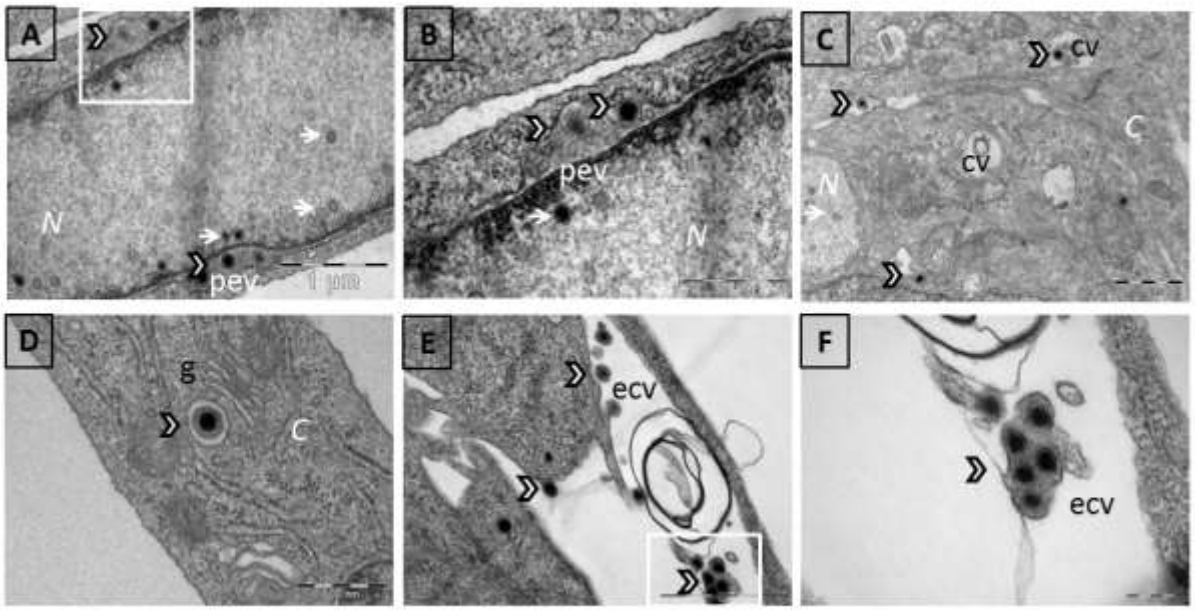

797

798 **Figure 3. TEM micrographs of CCB and KF-1 cells infected with Koi herpesvirus 5–7 dpi.**

799

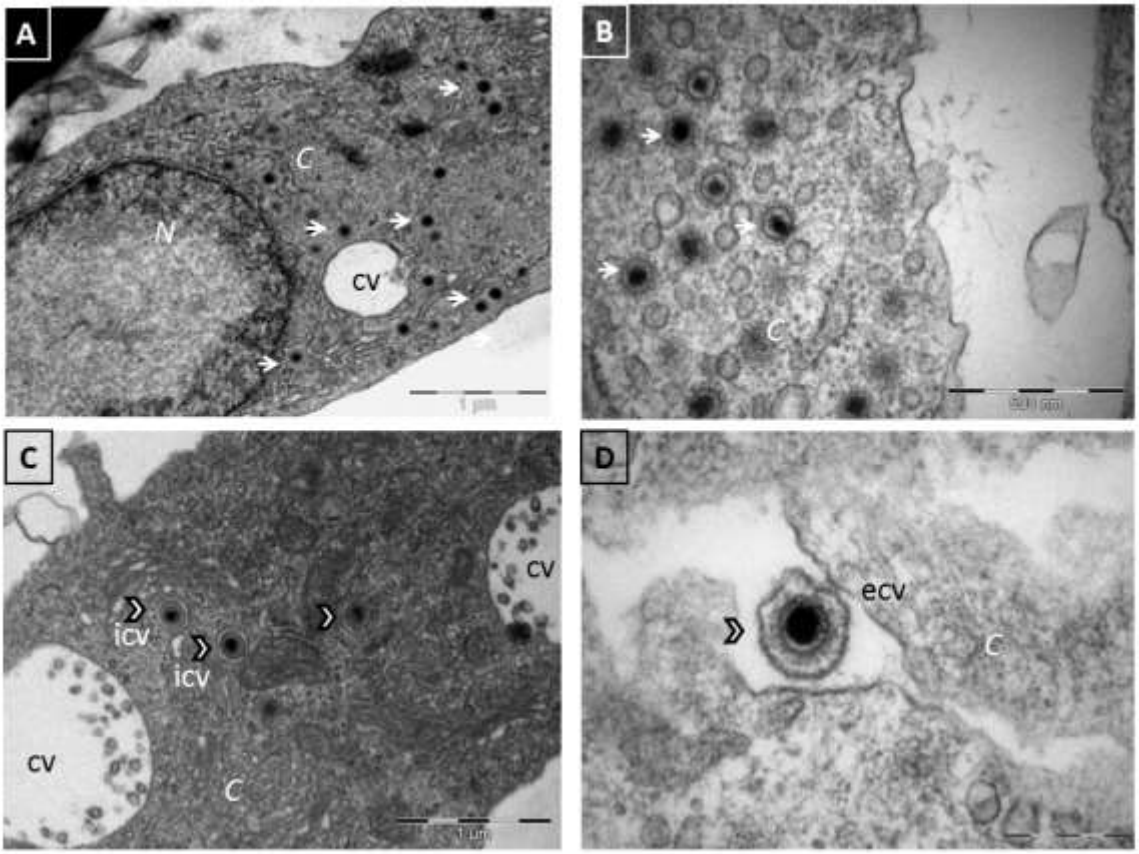

800

801 **Figure 4. TEM micrographs of CCB and KF-1 cells infected with Koi herpesvirus 5–7 dpi.**

802

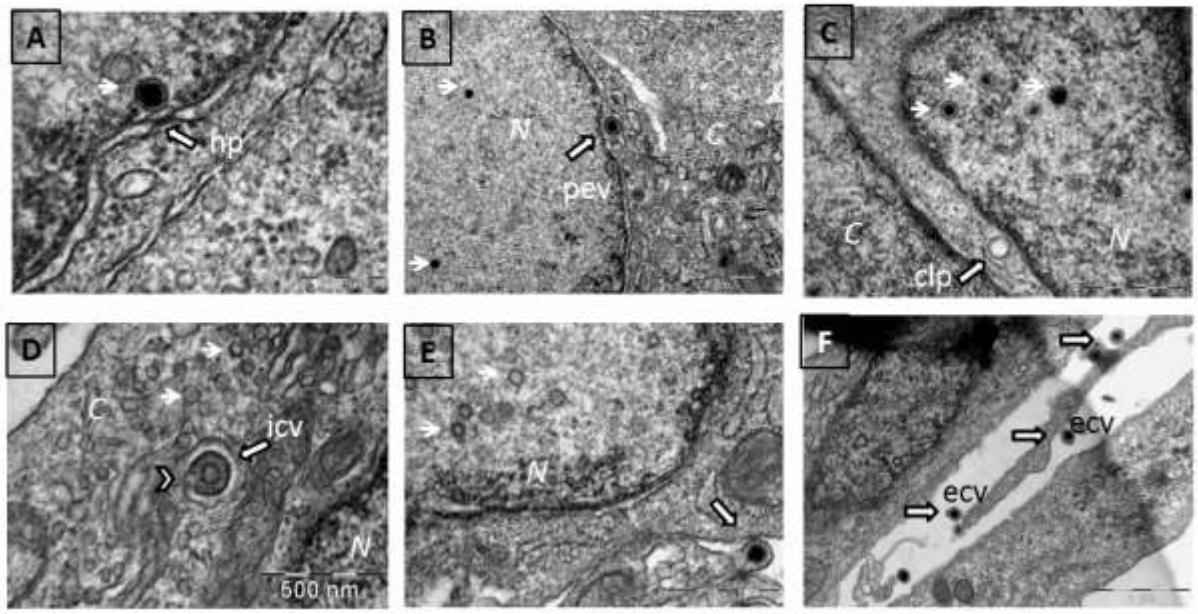

Figure 5. TEM micrographs of CyHV-3 virion morphogenesis and egress at membranous compartments.

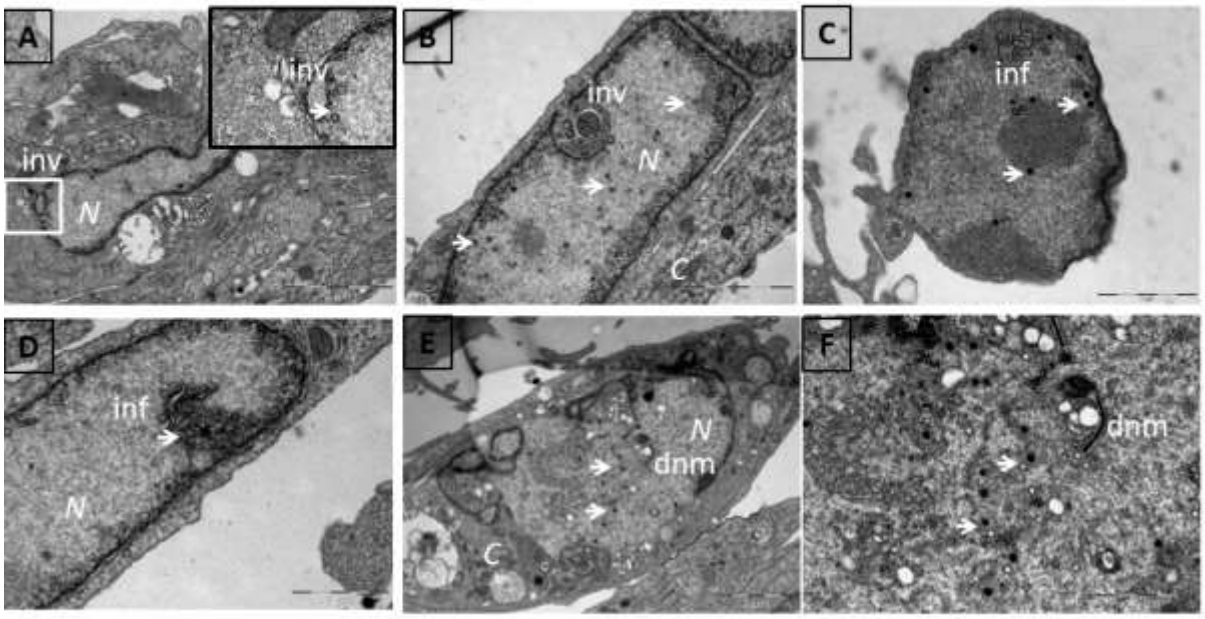

807

808 **Figure 6. TEM micrographs of CCB and KF-1 cells infected with Koi herpesvirus 5–7 dpi**
809 **showing various cytopathologies.**
810